

# Cytosolic protein delivery using ultrasound-guided vaporization of perfluorocarbon nano-droplets

Satoshi Yamaguchi<sup>1</sup>, Miho Kisaka<sup>1</sup>, Kotaro Higashi<sup>1</sup>, Ayumu Ishijima<sup>1</sup>, Takashi Azuma<sup>1</sup>, Keiichi Nakagawa<sup>1</sup>, Yoshikazu Shibasaki<sup>1</sup>, Ichiro Sakuma<sup>1</sup>, and Akimitsu Okamoto<sup>1</sup>

<sup>1</sup>The University of Tokyo

January 10, 2023

## Abstract

Ultrasound-guided protein delivery is promising for site-specific control of cellular functions in the deep interior of the body in a noninvasive manner. Herein, we propose a method for cytosolic protein delivery based on ultrasound-guided intracellular vaporization of perfluorocarbon nano-droplets. The nano-droplets were conjugated with cargo proteins through a bio-reductively cleavable linker and introduced into living cells via antibody-mediated binding to a cell-surface receptor, which gets internalized through endocytosis. After the cells were exposed to ultrasound for endosomal escape of proteins, the ultrasound-responsive cytosolic release of a cargo enzyme was confirmed by visualizing the hydrolysis of the fluorogenic substrate using confocal microscopy. Moreover, a significant decrease in cell viability was achieved via the release of a cytotoxic protein in response to ultrasound treatment. The results of this study provide the proof of a principle that protein-conjugated nano-droplets can be used as carriers in ultrasound-guided cytosolic delivery of proteins.

Submitted to **Biotechnology Journal** as a Research Article

## Cytosolic protein delivery using ultrasound-guided vaporization of perfluorocarbon nano-droplets

Satoshi Yamaguchi,<sup>1\*</sup> Miho Kisaka,<sup>1</sup> Kotaro Higashi,<sup>1</sup> Ayumu Ishijima,<sup>2</sup> Takashi Azuma,<sup>3</sup> Keiichi Nakagawa,<sup>2,5</sup> Yoshikazu Shibasaki,<sup>4</sup> Ichiro Sakuma<sup>2,5,6</sup> and Akimitsu Okamoto<sup>1\*</sup>

<sup>1</sup>Department of Chemistry & Biotechnology, The University of Tokyo, Tokyo, Japan

<sup>2</sup>Department of Precision Engineering, The University of Tokyo, Tokyo, Japan

<sup>3</sup>Center for Disease Biology and Integrative Medicine, The University of Tokyo, Tokyo, Japan

<sup>4</sup>Research Center for Advanced Science and Technology (RCAST), The University of Tokyo, Tokyo, Japan

<sup>5</sup>Department of Bioengineering, The University of Tokyo, Tokyo, Japan

<sup>6</sup>Medical Device Development and Regulation Research Center, The University of Tokyo, Tokyo, Japan

**Correspondence:** Satoshi Yamaguchi and Akimitsu Okamoto, Department of Chemistry & Biotechnology, The University of Tokyo, 7-3-1 Hongo, Bunkyo-ku, Tokyo 113-8656, Japan

**E-mail :** yamaguchi@chembio.t.u-tokyo.ac.jp or okamoto@chembio.t.u-tokyo.ac.jp

**Keywords:** protein delivery system, nano-droplets, ultrasound, mammalian cells, synthetic polymers

**Abbreviations:** **PCND**, phase-change nano-droplet; **EREG**, epiregulin; **PEG**, poly(ethylene glycol); **DPPC**, dipalmitoyl phosphatidylcholine; **DPPE**, dipalmitoyl phosphatidylethanolamine; **PFH**, perfluorohexane;  **$\beta$ -Gal**,  $\beta$ -galactosidase; **FDG**, fluorescein-di-( $\beta$ -D-galactopyranoside); **GSH**, reduced glutathione; **TAMRA**, tetramethyl rhodamine; **Sap**, Saporin; **PBS**, phosphate-buffered saline; **ME**, 2-mercaptoethanol; **Ex**, excitation wavelength; **Em**, emission wavelength; **Biotin-NHS**, Biotin N-succinimidyl ester; **DMEM**, Dulbecco’s modified Eagle’s medium.

## Abstract

Ultrasound-guided protein delivery is promising for site-specific control of cellular functions in the deep interior of the body in a noninvasive manner. Herein, we propose a method for cytosolic protein delivery based on ultrasound-guided intracellular vaporization of perfluorocarbon nano-droplets. The nano-droplets were conjugated with cargo proteins through a bio-reductively cleavable linker and introduced into living cells via antibody-mediated binding to a cell-surface receptor, which gets internalized through endocytosis. After the cells were exposed to ultrasound for endosomal escape of proteins, the ultrasound-responsive cytosolic release of a cargo enzyme was confirmed by visualizing the hydrolysis of the fluorogenic substrate using confocal microscopy. Moreover, a significant decrease in cell viability was achieved via the release of a cytotoxic protein in response to ultrasound treatment. The results of this study provide the proof of a principle that protein-conjugated nano-droplets can be used as carriers in ultrasound-guided cytosolic delivery of proteins.

## 1 | INTRODUCTION

Cytosolic protein delivery promisingly expands therapeutic possibilities<sup>[1,2]</sup>. The delivery of active proteins replaces disease-causing deficient or dysfunctional proteins that are important for essential cellular events<sup>[3]</sup>. Recently, the delivery of engineered proteins, such as CRISPR/Cas9, has been reported to artificially modulate genomic information, thereby opening a new window for therapeutic applications<sup>[4]</sup>. However, the development of precise and efficient technologies for cytosolic protein delivery remains challenging. As proteins are generally membrane-impermeable owing to their macromolecular nature and hydrophilic properties, most proteins cannot spontaneously enter the cells through cell membranes. Cell-permeable carriers consisting of peptides<sup>[5]</sup>, polymers<sup>[4,6-8]</sup>, liposomes<sup>[9,10]</sup>, and nanoparticles<sup>[11]</sup> have been actively employed to transport proteins inside cells. Although a few carriers have achieved direct cytosolic delivery of proteins by fusion with cellular plasma membranes<sup>[10,11]</sup>, most conventional carriers are usually taken up via endocytosis. Without being released from endosomes, cargo proteins are degraded in lysosomal compartments before being functional in the cytosol<sup>[2]</sup>. Therefore, technologies for endosomal escape have been developed by utilizing the proton sponge effect of pH-buffering agents, such as poly(ethyleneimine)<sup>[12]</sup> and a charge conversion block polymer<sup>[6]</sup>, by fusion of a carrier with the endosomal membrane<sup>[13]</sup> and by destabilization of the endosomal membrane with endosome-disruptive peptides<sup>[14,15]</sup>, polymers<sup>[7,16]</sup>, nanoparticles<sup>[11,17]</sup>, and photosensitizers<sup>[18-21]</sup>. Among these technologies, photochemical approaches offer photo-triggered spatiotemporal delivery of cargo proteins into the cytosol<sup>[19-22]</sup>. Selective cytosolic protein delivery at the desired timing and sites holds promise for safer and more effective therapies<sup>[1,22]</sup>. However, the light used during most photochemical reactions generally does not penetrate through the deeper areas of the body because of its low permeability in living tissues<sup>[23]</sup>.

Ultrasound readily penetrates deep into the interior of the body in a noninvasive manner<sup>[24]</sup>. Using focusing techniques, ultrasound exposure can be limited to a localized region, leading to selective exposure at the target site. Accordingly, ultrasound-responsive carriers for protein delivery have been reported to be promising non-invasive tools for spatiotemporal administration of proteins in deeper areas of the body<sup>[25-27]</sup>. However, no ultrasound-responsive carriers for cytosolic protein delivery have been reported till date. A method for ultrasound-induced drug release from endosomes has recently been reported<sup>[28]</sup>. In a pioneering study, liposomes containing fluorescent dyes and perfluorocarbon nano-droplets (phase-change nano-droplets, PCNDs) were introduced into living cells by folate-mediated endocytosis, and subsequent ultrasound-induced vaporization of PCNDs led to endosome rupture, thereby achieving escape of the dyes from the endosomes. In this study, we envisioned that endosomal rupture through vaporization of PCNDs could be applied to ultrasound-

induced cytosolic protein delivery. In our previous reports, PCNDs conjugated with an anti-epiregulin (EREG) antibody (named as 9E5) were taken up by high-EREG-expressing cancer cells via endocytosis<sup>[29]</sup> and were confirmed to vaporize inside the cells by exposure to ultrasound<sup>[30,31]</sup>. Therefore, 9E5-conjugated PCNDs were used as carriers for cytosolic protein delivery. Cargo proteins were conjugated with PCNDs via a bio-reductively cleavable disulfide linker. Protein-conjugated PCNDs were introduced into living cells via 9E5-mediated endocytosis, and after exposure to ultrasound, the cytosolic delivery of an enzyme and a cytotoxic protein was examined (Figure 1).

## 2 | RESULTS

### 2.1 | Design and synthesis of functionalized PEG-lipids

We designed and prepared PCNDs conjugated with cargo proteins and 9E5 using end-functionalized poly(ethylene glycol)(PEG)-lipids (Figure 1A and 1B). The PCNDs used in this study consisted of an outer lipid coating and an inner perfluorocarbon core. As previously reported<sup>[30,31]</sup>, dipalmitoyl phosphatidylcholine (DPPC) and its PEGylated analog (DPPE-PEG-OMe) were used as the basic lipid components (Figure 1B). Perfluorohexane (PFH) was employed as the perfluorocarbon based on a pioneering report on PCND-mediated endosomal rupture<sup>[28]</sup>. The lifetime of microbubbles generated from PCNDs with the PFH core was on the order of microseconds, and after ultrasound-induced vaporization, the bubbles were reported to disappear within 10  $\mu$ s by re-condensation<sup>[32]</sup>. Accordingly, in the reported endosomal rupture system, PCNDs were assumed to vaporize only for a moment inside the cells, thereby avoiding significant cell damage (Figure 1C)<sup>[28]</sup>. In our previous studies<sup>[30,31]</sup>, biotinylated antibody 9E5 was conjugated with biotinylated PEG-lipid (DPPE-PEG-biotin) by crosslinking with a streptavidin analog, NeutrAvidin, on the lipid coating of PCNDs (Figure 1B). Additionally, in this study, cargo proteins were designed to conjugate onto the PCND surface via a disulfide linker because they were required to be released in the reductive intracellular environment. Therefore, a PEG-lipid functionalized with 3-[(2-pyridyl) dithio] propionyl (DPPE-PEG-PyDTP) moiety was synthesized (see Supporting Information, Figure S1 and S2) and incorporated into the lipid coating of the PCNDs (Figure 1A). In the present design, the thiol group of the proteins reacted with DPPE-PEG-PyDTP, resulting in conjugation via thiol-disulfide exchange (Figure 1A).

### 2.2 | Conjugation and release of cargo proteins

To demonstrate the conjugation and reductive release of cargo proteins, a model enzyme, namely  $\beta$ -galactosidase ( $\beta$ -Gal), was conjugated with lipid-coated PFH droplets. After cleavage of the disulfide bond under a strong reductive condition and successive centrifugation, the amount of  $\beta$ -Gal released into the supernatant was detected by measuring the enzymatic activity with a fluorogenic substrate, namely fluorescein-di-( $\beta$ -D-galactopyranoside) (FDG). The enzymatic activity of the supernatants increased in response to the composition ratio of DPPE-PEG-PyDTP in the lipid coating of the droplets (see Supporting Information, Figure S3). This result suggested that  $\beta$ -Gal was conjugated with the droplets via disulfide bond formation with DPPE-PEG-PyDTP. Furthermore, the reductive release of  $\beta$ -Gal from the droplet surface was induced upon treatment with reduced glutathione (GSH), which results in a bio-reductive environment inside living cells. Reductive release of  $\beta$ -Gal was enhanced when using one to ten millimolar concentration of GSH (Figure 2A). A similar dependency on GSH concentration has been reported for conventional bio-reductive molecular tools that work in living cells<sup>[33]</sup>. From these results, the present conjugation method using DPPE-PEG-PyDTP was confirmed to be potentially suitable for intracellular protein release.

### 2.3 | Miniaturization and intracellular accumulation of droplets

Next, the lipid-coated PFH droplets were miniaturized and examined for uptake into living cells through endocytosis. The diameter of endosomes has been reported to be less than 120 nm<sup>[5]</sup>, and we wanted the droplets to be smaller than this. Therefore, the droplets were extruded through 30 nm pore filters, and their average diameter was determined to be 66.8 nm using dynamic light scattering (Figure 2B). The present PCNDs were modified with biotinylated and fluorescently labeled 9E5 through cross-linking with NeutrAvidin. Alexa Fluor 647 (AF647) was used for labeling 9E5. In addition, a fluorescently labeled PEG-lipid (tetramethyl rhodamine (TAMRA)-labeled PEG-lipid, DPPE-PEG-TAMRA) (Figure 1; also see

Supporting Information, Figure S1) was incorporated into the lipid coating of the droplets to visualize the PCNDs. In this study, human colon carcinoma DLD1 cells were used as the model EREG-expressing cancer cells. After the treatment of DLD1 cells with 9E5-conjugated PCNDs for 2 h at 37 °C, the fluorescence of both TAMRA and AF647 was observed using confocal fluorescence microscopy at almost the same location inside the cells (Figure 2C). In the case of non-conjugated PCNDs, no fluorescence was observed inside the cells (Figure 2D). These results indicate that the present PCNDs were taken up into living cells due to 9E5 conjugation, as previously reported<sup>[30,31]</sup>.

#### 2.4 | Υλτρασουνδ-ινδυσεδ ςψτοσολις δελιερψ οφ β-Γαλ

To demonstrate ultrasound-induced cytosolic delivery of proteins, β-Gal was carried into DLD1 cells by conjugation with 9E5-conjugated PCNDs. After the intracellular accumulation of PCNDs carrying β-Gal, the cells were exposed to ultrasound using previously reported experimental setup<sup>[30]</sup>. The cytosolic release of β-Gal was visualized using a fluorogenic substrate, namely TokyoGreen-βGal (TG-βGal)<sup>[34]</sup>. In addition, to visualize endosomes and lysosomes in the endocytosis pathway, the cells were stained with LysoTracker<sup>®</sup> Blue, which helps in visualizing acidic organelles. In ultrasound-exposed cells, green fluorescence derived from the hydrolysis of TG-βGal was observed throughout the intracellular area (Figure 3A), as previously reported in β-Gal-expressing cells<sup>[34]</sup>. This result clearly showed that β-Gal was released into the cytosol. In contrast, in non-ultrasound-exposed cells, fluorescence was observed only in endosomes and lysosomes (Figure 3B). Similarly, cytosolic fluorescence was not observed in the control cells, which were treated with PCNDs without β-Gal after the ultrasound treatment (Figure 3C); the fluorescence was also not observed in the untreated cells (Figure 3D). This result clearly indicated that β-Gal was released from the endocytosis pathway into the cytosol in response to ultrasound treatment.

#### 2.5 | Ultrasound-induced cytosolic delivery of Saporin

Finally, we demonstrated a control over cells in an ultrasound-induced manner using the current cytosolic protein delivery system. Saporin (Sap) was used as a cargo protein. Sap is a plant-derived ribosome-inactivating protein that leads to cell death through its introduction into the cytosol<sup>[35,36]</sup>. Sap has no free thiol group; therefore, the amine group of the lysine residues was thiolated with 2-iminothiolane hydrochloride<sup>[37,38]</sup>. Thiolated Sap was conjugated with PCNDs via disulfide bond formation in the same manner as that used for β-Gal. After intracellular accumulation of PCNDs carrying Sap, the cells were exposed to ultrasound, followed by incubation for 2 days. Alive cells were stained with calcein-AM, and all cells were subsequently analyzed for the presence of green fluorescence of calcein using flow cytometry. The cell viability drastically decreased to below 30% after the treatment with both Sap-carrying PCNDs and ultrasound, while the treatment with Sap-carrying PCNDs without exposure to ultrasound barely reduced the cell viability (Figure 4). Although the cell viability decreased to 66% even in the control experiment wherein PCNDs without Sap were used, there was a significant difference in the cell viability between PCNDs with and without Sap after an exposure to ultrasound. These results indicated that Sap was released into the cytosol upon exposure to ultrasound, resulting in a significant contribution to decreased cell viability.

### 3 | DISCUSSION

For ultrasound-induced endosomal escape, both destabilization of the endosomal membrane and protein release from the carriers are required. In this study, to meet the former requirement, PCNDs were employed as an ultrasonically endosome-disruptive carrier based on a pioneering study<sup>[28]</sup>. To meet the later requirement, a disulfide-linked material for the bio-reductive release of proteins was developed in this study. This material was confirmed to conjugate with a model protein with the lipid coating of droplets and to release it in response to reductive conditions *in vitro* (Figure 2A). Even in living cells, the bio-reductive release of β-Gal and Sap was strongly suggested by the hydrolysis of the fluorogenic substrate in the cytosol (Figure 3) and enhancement in cytotoxicity (Figure 4), respectively. Furthermore, cytosolic delivery of these two model proteins was observed in an ultrasound-responsive manner (Figure 3 and 4). This result indicates that endosomal escape of cargo proteins was achieved by vaporization of PCNDs.

In our previous works, intracellular vaporization of antibody-conjugated PCNDs was utilized for ultrasound-

dependent induction of cell death to targeted cells<sup>[30,31]</sup>. Different from the present study, the PCNDs which included the equal mixture of PFH (boiling point = 57 °C) and perfluoropentane (PFP, boiling point = 29 °C) was employed. Here, employment of inner perfluorocarbons with a low boiling point increases the size and the lifetime of bubbles after vaporization, leading to remaining and coalescence of bubbles<sup>[28]</sup>. Such properties of PCNDs with a lower boiling point are desirable in intracellular vaporization for enhancing cytotoxicity, and therefore, the PCNDs including the PFH-PFP mixture was employed in the previous works<sup>[30,31]</sup>. In the present study for cytosolic protein delivery, the PCNDs including PFH only was employed for suppressing cytotoxicity of their vaporization. Actually, in  $\beta$ -Gal delivery, no significant cell damage was observed in the microscopic images one hour after ultrasound exposure (Fig. 3), as observed in the pioneering study in which the PCNDs including PFH only were used<sup>[28]</sup>. This result is quite different from the images in our previous works in which cells were disrupted and detached from the dish surface by PCND vaporization<sup>[30]</sup>. However, in Sap delivery, the vaporization of PCNDs without carrying Sap caused non-negligible cytotoxicity after incubation for 48 h (Figure 4). In our previous work, the cell viability after vaporization of PCNDs was influenced by the PCND concentration during cellular uptake and the experimental setup for ultrasound exposure<sup>[31]</sup>. Further optimization of these conditions is required to manipulate cell functions without causing cell damage. Thus, although there is a room for improvement, we have demonstrated a proof-of-principle that ultrasound-dependent cytosolic protein delivery is possible using chemically functionalized PCNDs.

In conclusion, the protein-conjugated PCNDs could be used for ultrasound-induced cytosolic protein delivery. Through the development of a thiol-reactive lipid coating, cargo proteins were carried on the droplets through a bio-reductive disulfide linkage. When the cargo protein had no thiol group, it was conjugated with the droplets through reversible thiolation of the amine groups. In principle, the proposed method can be applied to any protein. These protein-conjugated PCNDs were taken up into living cells, and after ultrasound exposure, the cargo proteins functioned in the cytosol in an ultrasound-induced manner, probably because of endosomal escape by the vaporization of the droplets in the endosomal pathway. In this study, by utilizing an anti-cancer antibody as the molecular device for intracellular delivery, protein-conjugated PCNDs were accumulated in cancer cells. Similarly, according to the objectives, proteins can be selectively delivered into the cytosol of various targeted cells by employing the desired targeting ligands. Furthermore, based on the double targeting effect of both ultrasound and the ligands, the current method of cytosolic delivery is expected to meet a wide variety of demands in fundamental studies and therapeutic uses.

## 4 | EXPERIMENTAL SECTION

### 4.1 | Synthesis of PEG-lipid derivatives

End-functionalized PEG-lipids, such as DPPE-PEG-OMe, DPPE-PEG-TAMRA, DPPE-PEG-biotin, and DPPE-PEG-PyDTP, were synthesized from commercially available bifunctionalized PEGs and DPPE (Figure 1A and 1B; also see Supporting Information Figure S1 and S2). Details of the synthesis are provided in the Supporting Information. All products were identified using <sup>1</sup>H-NMR spectroscopy.

### 4.2 | Preparation of perfluorocarbon droplets

DPPE and PEG-lipid derivatives of various compositions (8  $\mu$ mol in total) were dissolved in CH<sub>2</sub>Cl<sub>2</sub>. The solvent was evaporated to form a lipid film, which was then suspended in PBS (1 ml) using a bath sonicator to prepare liposomes. After three cycles of freezing in liquid nitrogen and thawing in a water bath (55 °C), 17  $\mu$ l of PFH was added to the liposome suspension, and the mixture was sonicated on ice using a probe sonicator (UD-200; TOMY Digital Biology Co., Ltd., Tokyo, Japan) to form PFH droplets. After centrifugation (3000  $\times g$ ) at 4 °C for 5 min, the supernatant was removed, and the precipitates were resuspended in 20% glycerol PBS solution. This droplet suspension was frozen and stored in a freezer (-20 degC) until further use.

### 4.3 | δνθυγατιον ανδ ρελεασε οφ β-Γαλ ωιτη/φρομ δροπλετς

Droplets with various DPPE-PEG-PyDTP concentrations were prepared as described above (see Supporting Information Table S1). After centrifugation, the precipitate containing the droplets in a microtube was suspended in  $\beta$ -Gal solution (1  $\mu$ M in 1 mM MgCl<sub>2</sub>-PBS solution) and mechanically rotated in a refrigerator

(4 °C) for 1 h. After centrifugation, the supernatant was removed, and the precipitate was resuspended in PBS. The process of centrifugation followed by the removal of supernatant and resuspension in PBS was repeated four times to remove the free  $\beta$ -Gal. For the reductive release assay,  $\beta$ -Gal-conjugated droplets were suspended in 200  $\mu$ l of GSH solution (various concentrations from 0.010 mM to 10 mM in PBS) followed by incubation for 2 h. After centrifugation, the supernatant was recovered, desalted, freeze-dried, and rehydrated in 10  $\mu$ l of 1.0 mM  $MgCl_2$ -PBS solution. Subsequently, 4  $\mu$ l of the solution was added to 116  $\mu$ l of fluorogenic substrate solution (0.10 mM FDG, 1.0 mM  $MgCl_2$ , and 112 mM ME in PBS), and then, the time-course of fluorescent intensity (Ex: 490 nm, Em: 514 nm) was assessed using a plate reader (Cytation<sup>TM</sup> 5, Biotek Instruments, Vermont, USA).  $\beta$ -Gal concentration was determined based on the rate of increase in fluorescence.

#### 4.4 | Droplet extrusion

The droplet suspension was extruded 30 times through 30 nm pore filters (Nuclepore Track-Etch Membrane, Whatman Inc., NY, USA) using an extruder (Avestin Inc., Mannheim, Germany) to prepare PCNDs. The mean droplet diameter was measured using a Zetasizer Nano-ZS (Malvern Instruments Ltd., Malvern, UK).

#### 4.5 | Cell culture

Human colon carcinoma DLD1 cells were purchased from JCRB Cell Bank (National Institutes of Biomedical Innovation, Health and Nutrition, Osaka, Japan) and cultured in a culture medium (RPMI1640 supplemented with 10% FBS and 0.1% penicillin/streptomycin) at 37 °C in a humidified atmosphere containing 5%  $CO_2$ .

#### 4.6 | Introduction of fluorescence-labeled PCNDs into cells

To microscopically observe the intracellular accumulation of PCNDs, PCNDs were modified with fluorescence-labeled 9E5 and fluorescence-labeled PEG-lipid. 9E5 was prepared using 9E5-expressing hybridoma cells<sup>[31,32]</sup> and biotinylated by reacting with biotin-NHS (13 eq), which was synthesized as previously reported<sup>[39]</sup>. After purification with a gel filtration column, biotinylated 9E5 was fluorescently labeled by allowing it to react with Alexa647-NHS (10 eq). Biotinylated and fluorescently labeled 9E5 was purified by gel filtration and then was conjugated with PCNDs, as previously reported<sup>[30,31]</sup>. Here, PCNDs were prepared using DPPC, DPPE-PEG-OMe, DPPE-PEG-biotin, and DPPE-PEG-TAMRA. Biotinylated and fluorescently labeled 9E5 was mixed with NeutrAvidin for 15 min at room temperature to prepare the 9E5-NeutrAvidin conjugate. PCNDs were suspended in 9E5-NeutrAvidin solution and incubated for 30 min on ice for modification with 9E5. After centrifugation at  $3000 \times g$  for 5 min, the PCND pellet was washed with cold PBS and suspended in RPMI-based culture medium. DLD1 cells were treated with 9E5-conjugated PCND suspension for 3 h under culture conditions. After washing the dish surface, the cells were observed using a confocal laser-scanning microscope (LSM 510 META; Carl Zeiss, Germany) equipped with a  $20\times$  objective lens. The fluorescence of TAMRA (Em: 560/610 nm) and AF647 (Em:650/680 nm) was observed using excitation lasers at wavelengths of 552 and 633 nm, respectively.

#### 4.7 | Ιντρασελλυλαρ δελιερχ οφ $\beta$ -Γαλ

PCNDs were prepared using DPPC, DPPE-PEG-OMe, DPPE-PEG-biotin, and DPPE-PEG-PyDTP as the lipid coating and suspended in 1  $\mu$ M  $\beta$ -Gal solution, followed by mechanical rotation in a refrigerator (4 °C) for 1 h. After centrifugation and washing, 9E5-conjugation for the PCNDs was performed as described above. After centrifugation and washing,  $\beta$ -Gal- and 9E5-conjugated PCNDs were suspended in RPMI1640-based culture medium. DLD1 cells were treated with  $\beta$ -Gal- and 9E5-conjugated PCND suspension for 3 h under culture conditions. After washing the dish surface, the cells were exposed to ultrasound (5 MHz) using a previously reported method<sup>[30,31]</sup>. After ultrasound exposure, the cells were stained with TG- $\beta$ Gal and LysoTracker Blue for 1 h under culture conditions. After washing the dish surface, the cells were observed under a confocal microscope, as described above. The fluorescence of TG- $\beta$ Gal (Em: 505/525 nm) and LysoTracker Blue (Em: 410/460 nm) was observed using excitation lasers at wavelengths of 488 and 405 nm, respectively.

#### 4.8 | Intracellular delivery of Sap

Sap was thiolated by reacting it with 2-iminothiolane hydrochloride (25 eq) for 1.5 h on ice<sup>[37,38]</sup>. PCNDs were suspended in thiolated Sap solution (2  $\mu$ M), followed by mechanical rotation in a refrigerator (4 °C) overnight. After washing, Sap-conjugated PCNDs were modified with 9E5-NeutrAvidin conjugates, as described above. DLD1 cells were treated with Sap- and 9E5-conjugated PCND suspension for 3 h. PCND-treated cells were exposed to ultrasound, as described above. After ultrasound exposure, the cells were cultured for 48 h and then stained with calcein-AM. The cells were harvested from the dish using 0.25% trypsin-EDTA and analyzed using a flow cytometer (Guava easyCyte 8; Luminex Japan Co. Ltd., Tokyo, Japan).

## NOVELTY STATEMENT

We have demonstrated that PCNDs carrying cargo proteins achieve cytosolic protein delivery in an ultrasound-guided manner. To achieve enhanced therapeutic effects and reduced side effects in protein drug treatment, an ultrasound-responsive carrier is promising because focused ultrasound readily penetrates deep into the body in a non-invasive manner and only a limited region is exposed to ultrasound. For endosomal escape of cargo proteins, we employed PCNDs as carriers to destabilize the endosomal membrane via ultrasound-induced vaporization of PCNDs in endosomes. To date, no protein has been reported to be released from endosomes by utilizing PCND vaporization. Here, we designed and synthesized a novel PEG-lipid that can conjugate with any cargo protein on the lipid coating of the droplets through disulfide bond formation because it is required that cargo proteins be released from the carrier in the reductive cytosol. In this study, both cargo proteins with and without free thiols in their wild type forms were released in the cytosol in response to ultrasound by utilizing reversible protein thiolation in the absence of thiol. Thus, our study clearly shows the proof of a principle that PCNDs are versatile carriers for ultrasound-guided cytosolic protein delivery.

## ACKNOWLEDGMENTS

This work was supported by the Ministry of Education, Culture, Sports, Science, and Technology Grant-in-Aid for Scientific Research (C) 15K06575 and the Translational Systems Biology and Medicine Initiative (TSBMI). This work was supported in part by Japan Science and Technology Agency (JST) CREST Grant Number JPMJCR1902.

## CONFLICT OF INTEREST

The authors declare no financial or commercial conflicts of interest.

## DATA AVAILABILITY STATEMENT

The data supporting the findings of this study are available from the corresponding author upon a reasonable request.

## REFERENCES

1. Gu, Z., Biswas, A., Zhao, M., Tang, Y. (2011). Tailoring nanocarriers for intracellular protein delivery. *Chemical Society Review* , *40* , 3638-3655. <https://doi.org/10.1039/c0cs00227e>
2. Goswami, R., Jeon, T., Nagaraj, H., Zhai, S., Rotello, V. M. (2020). Accessing intracellular targets through nanocarrier-mediated cytosolic protein delivery. *Trends Pharmacol Science* , *41* , 743-754. <https://doi.org/10.1016/j.tips.2020.08.005>
3. Lv, J., Fan, Q., Wang, H., Cheng, Y. (2019). Polymers for cytosolic protein delivery. *Biomaterials* , *218* , 119358. <https://doi.org/10.1016/j.biomaterials.2019.119358>.
4. Liu, C., Wan, T., Wang, H., Zhang, S., Ping, Y., Cheng, Y. (2019). A boronic acid-rich dendrimer with robust and unprecedented efficiency for cytosolic protein delivery and CRISPR-Cas9 gene editing. *Science Advances* , *5* , eaaw8922. <https://doi.org/10.1126/sciadv.aaw8922>
5. Futaki, S., Nakase, I. (2017). Cell-surface interactions on arginine-rich cell-penetrating peptides allow for multiplex modes of internalization. *Accounts of Chemical Research* , *50* , 2449-2456.

<https://doi.org/10.1021/acs.accounts.7b00221>

6. Lee, Y., Ishii, T., Cabral, H., Kim, H. J., Seo, J.-H., Nishiyama, N., Oshima, H., Osada, K., Kataoka, K. (2009). Charge-conversional polyionic complex micelles-efficient nanocarriers for protein delivery into cytoplasm. *Angewandte Chemie International Edition* , 48, 5309-5312. <https://doi.org/10.1002/anie.200900064>
7. Du, S., Liew, S. S., Li, L., Yao, S. Q. (2018). Bypassing endocytosis: direct cytosolic delivery of proteins. *Journal of the American Chemical Society* , 140, 15986-15996. <https://doi.org/10.1021/jacs.8b06584>
8. Mogaki, R., Hashim, P. K., Okuro, K., Aida, T. (2017). Guanidinium-based “molecular glues” for modulation of biomolecular functions. *Chemical Society Review* , 46 , 6480-6491. <https://doi.org/10.1039/c7cs00647k>
9. Kube, S., Hersch, N., Naumovska, E., Gensch, T., Hendriks, J., Franzen, A., Landvogt, L., Siebrasse, J. P., Kubitschek, U., Hoffmann, B., Merkel, R., Csiszar, A. (2017). Fusogenic liposomes as nanocarriers for the delivery of intracellular proteins. *Langmuir* , 33 , 1051-1059. <https://doi.org/10.1021/acs.langmuir.6b04304>
10. Yang, J., Tu, J., Lamers, G. E. M., Olsthoorn, R. C. L., Kros, A. (2017). Membrane fusion mediated intracellular delivery of lipid bilayer coated mesoporous silica nanoparticles. *Advanced Healthcare Materials* , 6 , 1700759. <https://doi.org/10.1002/adhm.201700759>
11. Scaletti, F., Hardie, J., Lee, Y.-W., Luther, D. C., Ray, M., Rotello, V. M. (2018). Protein delivery into cells using inorganic nanoparticle-protein supramolecular assemblies. *Chemical Society Review* , 47 , 3421–3432. <https://doi.org/10.1039/c8cs00008e>
12. Futami, J., Kitazoe, M., Maeda, T., Nukui, E., Sakaguchi, M., Kosaka, J., Miyazaki, M., Kosaka, M., Tada, H., Seno, M., Sasaki, J., Huh, N.-H., Namba M., Yamada, H. (2005) Intracellular delivery of proteins into mammalian living cells by polyethylenimine-cationization. *Journal of Bioscience Bioengineering* , 99 , 95–103. <https://doi.org/10.1263/jbb.99.95>
13. Liu, B., Ejaz, W., Gong, S., Kurbanov, M., Canakci, M., Anson, F., Thayumanavan, S. (2020). Engineered interactions with mesoporous silica facilitate intracellular delivery of proteins and gene editing. *Nano Letters* , 20 , 4014–4021. <https://doi.org/10.1021/acs.nanolett.0c01387>
14. Nakase, I., Kobayashi, S., Futaki, S. (2010). Endosome-disruptive peptides for improving cytosolic delivery of bioactive macromolecules. *Peptide Science* , 94 , 763–770. <https://doi.org/10.1002/bip.21487>
15. Yao, P., Zhang, Y., Meng, H., Sun, H., Zhong, Z. (2019). Smart polymersomes dually functionalized with cRGD and fusogenic GALA peptides enable specific and high-efficiency cytosolic delivery of apoptotic proteins. *Biomacromolecules* , 20 , 184-191. <https://doi.org/10.1021/acs.biomac.8b01243>
16. Liu, C., Shen, W., Li, B., Li, T., Chang, H., Cheng, Y. (2019). Natural polyphenols augment cytosolic protein delivery by a functional polymer. *Chemistry of Materials*, 31 , 1956-1965. <https://doi.org/10.1021/acs.chemmater.8b04672>
17. Das, P., Jana, N. R. (2016). Length-controlled synthesis of calcium phosphate nanorod and nanowire and application in intracellular protein delivery. *ACS Applied Materials Interfaces* , 8 , 8710-8720. <https://doi.org/10.1021/acsami.6b01667>
18. Berg, K., Selbo, P. K., Prasmickaite, L., Tjelle, T. E., Sandvig, K., Moan, J., Gaudernack, G., Fodstad, O., Kjolsrud, S., Anholt, H., Rodal, G. H., Rodal, S. K., Hogset, A. (1999). Photochemical internalization: a novel technology for delivery of macromolecules into cytosol. *Cancer Research* , 59 , 1180–1183.
19. Matsushita, M., Noguchi, H., Lu, Y.-F., Tomizawa, K., Michiue, H., Li, S.-T., Hirose, K., Bonner-Weir, S., Matsui, H. (2004). Photo-acceleration of protein release from endosome in the protein transduction system. *FEBS Letters* , 572 , 221–226. <https://doi.org/10.1016/j.febslet.2004.07.033>
20. Minamihata, K., Maeda, Y., Yamaguchi, S., Ishihara, W., Ishiwatari, A., Takamori, S., Yamahira, S., Nagamune, T. (2015). Photosensitizer and polycationic peptide-labeled streptavidin as a nano-

carrier for light-controlled protein transduction. *Journal of Bioscience Bioengineering* , 120 , 630–636. <https://doi.org/10.1016/j.jbiosc.2015.04.001>

21. Soe, T. H., Watanabe K., Ohtsuki, T. (2021). Photoinduced endosomal escape mechanism: a view from photochemical internalization mediated by CPP-photosensitizer conjugates. *Molecules* , 26 , 36. <https://doi.org/10.3390/molecules26010036>

22. Li, Y., Zhou, Y., Wang, T., Long, K., Zhang, Y., Wang, W. (2021). Photoenhanced cytosolic protein delivery based on a photocleavable group-modified dendrimer. *Nanoscale* , 13 , 17784–17792. <https://doi.org/10.1039/d1nr04430c>

23. Eichler, J., Knof, J., Lenz, H. (1977). Measurements on the depth of penetration of light (0.35–1.0 microgram) in tissue. *Radiation and Environmental Biophysics* , 14 , 239–242. <https://doi.org/10.1007/BF01323942>

24. Tang, H., Zheng, Y., Chen, Y. (2017). Materials chemistry of nanoultrasonic biomedicine. *Advanced Materials* , 29 , 1604105. <https://doi.org/10.1002/adma.201604105>

25. Uesugi, Y., Kawata, H., Jo, J., Saito, Y., Tabata, Y. (2010). An ultrasound-responsive nano delivery system of tissue-type plasminogen activator for thrombolytic therapy. *Journal of Controlled Release* , 147 , 269–277. <https://doi.org/10.1016/j.jconrel.2010.07.127>

26. Huebsch, N., Kearney, C. J., Zhao, X., Kim, J., Cezar, C. A., Suo, Z., Mooney, D. J. Ultrasound-triggered disruption and self-healing of reversibly cross-linked hydrogels for drug delivery and enhanced chemotherapy. *Proceedings of the National Academy of Sciences of the United States of America* , 111 , 9762–9767. <https://doi.org/10.1073/pnas.1405469111>

27. Yamaguchi, S., Higashi, K., Azuma, T., Okamoto, A. (2019). Supramolecular polymeric hydrogels for ultrasound-guided protein release. *Biotechnology Journal* , 14 , 1800530. <https://doi.org/10.1002/biot.201800530>

28. Lattin, J. R., Javadi, M., McRae, M., Pitt, W. G. (2015). Cytosolic delivery via escape from the endosome using emulsion droplets and ultrasound. *Journal of Drug Targeting* , 23 , 469–479. <https://doi.org/10.3109/1061186X.2015.1009074>

29. Lee, Y.-H., Iijima, M., Kado, Y., Mizohata, E., Inoue, T., Sugiyama, A., Doi, H., Shibasaki, Y., Kodama, T. (2013). Construction and characterization of functional anti-epiregulin humanized monoclonal antibodies. *Biochemical Biophysical Research Communications* , 441 , 1011–1017. <https://doi.org/10.1016/j.bbrc.2013.11.014>

30. Ishijima, A., Minamihata, K., Yamaguchi, S., Yamahira, S., Ichikawa, R., Kobayashi, E., Iijima, M., Shibasaki, Y., Azuma, T., Nagamune, T., Sakuma, I. (2017). Selective intracellular vaporisation of antibody-conjugated phase-change nano-droplets in vitro. *Scientific Reports* , 7 , 44077. <https://doi.org/10.1038/srep44077>

31. Ishijima, A., Yamaguchi, S., Azuma, T., Kobayashi, E., Shibasaki, Y., Nagamune, T., Sakuma, I. (2019). Selective intracellular delivery of perfluorocarbon nanodroplets for cytotoxicity threshold reduction on ultrasound-induced vaporization. *Cancer Reports* , 2 , e1165. <https://doi.org/10.1002/cnr2.1165>

32. Ishijima, A., Tanaka, J., Azuma, T., Minamihata, K., Yamaguchi, S., Kobayashi, E., Nagamune, T., Sakuma, I. (2016). The lifetime evaluation of vapourised phase-change nano-droplets. *Ultrasonics* , 69 , 97–105. <https://doi.org/10.1016/j.ultras.2016.04.002>

33. Qian, L., Fu, J., Yuan, P., Du, S., Huang, W., Li, L., Yao, S. Q. (2018). Intracellular delivery of native proteins facilitated by cell-penetrating poly(disulfide)s. *Angewandte Chemie International Edition* , 130 , 1548–1552. <https://doi.org/10.1002/ange.201711651>

34. Urano, Y., Kamiya, M., Kanda, K., Ueno, T., Hirose, K., Nagano, T. (2005). Evolution of fluorescein as a platform for finely tunable fluorescence probes. *Journal of the American Chemical Society* , *127* , 4888-4894. <https://doi.org/10.1021/ja043919h>
35. Stirpe, F., Gasperi-Campani, A., Barbieri, L., Falasca, A., Abbondanza, A., Stevens, W. A. (1983). Ribosome-inactivating proteins from the seeds of *Saponaria officinalis* L., of *Agrostemma githago* L., and of *Asparagus officinalis* L., and from the latex of *Hura crepitans* L. *Biochemical Journal* , *216* , 617-625. <https://doi.org/10.1042/bj2160617>
36. Yamaguchi, S., Yamamoto, K., Yamamoto, R., Takamori, S., Ishiwatari, A., Minamihata, K., Nagamune, T., Okamoto, A. (2022). Intracellular protein photoactivation using sterically bulky caging. *ChemBioChem* , *23* , e202200476. <https://doi.org/10.1002/cbic.202200476>
37. Ishiwatari, A., Yamaguchi, S., Takamori, S., Yamahira, S., Minamihata, K., Nagamune, T. (2016). Photolytic protein aggregates: versatile materials for controlled release of active proteins. *Advanced Healthcare Materials* , *5* , 1002-1007. <https://doi.org/10.1002/adhm.201500957>
38. Yamaguchi, S., Takamori, S., Yamamoto, K., Ishiwatari, A., Minamihata, K., Yamada, E., Okamoto, A., Nagamune, T. (2021). Sterically bulky caging of transferrin for photoactivatable intracellular delivery. *Bioconjugate Chemistry* , *32* , 1535-1540. <https://doi.org/10.1021/acs.bioconjchem.1c00159>
39. Yamaguchi, S., Ohashi, N., Minamihata, K., Nagamune, T. (2021). Photodegradable avidin-biotinylated polymer conjugate hydrogels for cell manipulation. *Biomaterials Science* , *9* , 6416-6424. <https://doi.org/10.1039/d1bm00585e>

## Figure captions

**Figure 1.** Schematic illustration depicting cytosolic protein delivery using ultrasound-guided vaporization of phase-change nano-droplets. (A) The chemical structure of the protein anchoring reagent that anchors the protein onto the nano-droplets (DPPE-PEG-PyDTP) and the corresponding anchoring reaction. (B) Chemical structures of the nano-droplet modifiers for antibody modification (DPPE-PEG-Biotin), stabilization (DPPE-PEG-OMe), and labeling (DPPE-PEG-TAMRA). (C) Schematic of cellular uptake and ultrasound-guided intracellular vaporization of the droplets carrying cargo proteins for cytosolic delivery through endosomal escape.

**Figure 2.** Characterization of droplets for cytoplasmic protein delivery. (A) The concentration of the released  $\beta$ -galactosidase from the droplets after incubation with various concentrations of reduced glutathione (GSH). (B) Dynamic light scattering intensity of the droplets after down-sizing using an extruder. (C) Confocal microscopic images of DLD1 cells treated with nano-droplets modified with anti-epiregulin antibody and (D) without anti-epiregulin antibody. The antibody was labeled with a fluorescent dye (Alexa Fluor 647: AF647) (pink). The nano-droplets were labeled with DPPE-PEG-TAMRA (orange). Scale bar: 10  $\mu$ m.

**Figure 3.** Fluorescence confocal microscopic images of cells after ultrasound-induced cytosolic delivery of  $\beta$ -galactosidase ( $\beta$ -Gal). (A) DLD1 cells treated with phase-change nano-droplets (PCNDs) carrying  $\beta$ -Gal and ultrasound, (B) those treated with  $\beta$ -Gal-carrying PCNDs without ultrasound, and (C) those treated with PCNDs not carrying  $\beta$ -Gal and ultrasound were observed after staining with a fluorescent substrate for  $\beta$ -Gal (TokyoGreen- $\beta$ Gal) and an endosomal and lysosomal staining dye (Lysotracker). (D) Intact cells were also observed as the control in the same way. The fluorescence images for TokyoGreen- $\beta$ Gal (green) and Lysotracker (cyan) were merged along with the differential interference contrast images. Scale bar: 25  $\mu$ m.

**Figure 4.** Viabilities of cells after ultrasound (US)-induced cytosolic delivery of saporin (Sap). DLD1 cells were treated with the nano-droplets (PCNDs) with or without Sap and then were exposed to ultrasound (US) or not. In the same way, the viability of intact cells was examined. The viability was normalized to that of the intact cells. Each bar represents the mean  $\pm$  S.E. (n = 3). \*p < 0.01 and \*\*p < 0.05 versus the cells treated with both PCNDs carrying Sap and US (t-test).

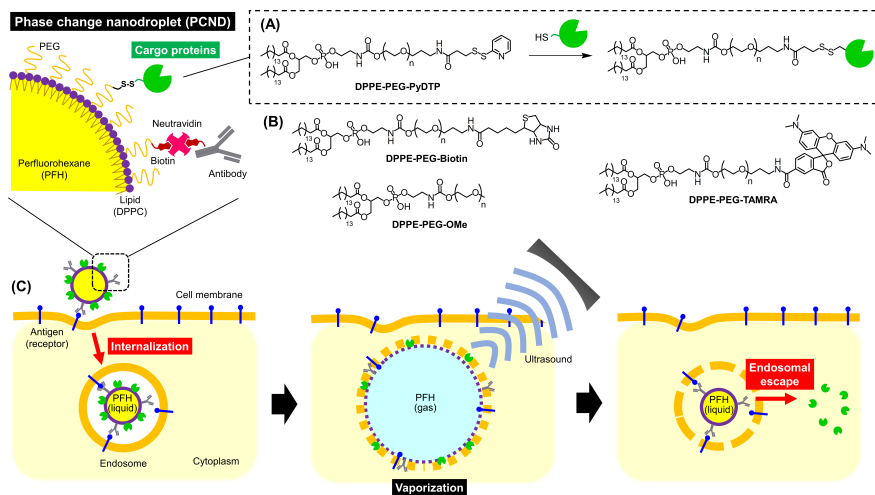


**Figure 1.** Schematic illustration depicting cytosolic protein delivery using ultrasound-guided vaporization of phase-change nano-droplets. (A) The chemical structure of the protein anchoring reagent that anchors the protein onto the nano-droplets (DPPE-PEG-PyDTP) and the corresponding anchoring reaction. (B) Chemical structures of the nano-droplet modifiers for antibody modification (DPPE-PEG-Biotin), stabilization (DPPE-PEG-OMe), and labeling (DPPE-PEG-TAMRA). (C) Schematic of cellular uptake and ultrasound-guided intracellular vaporization of the droplets carrying cargo proteins for cytosolic delivery through endosomal escape.

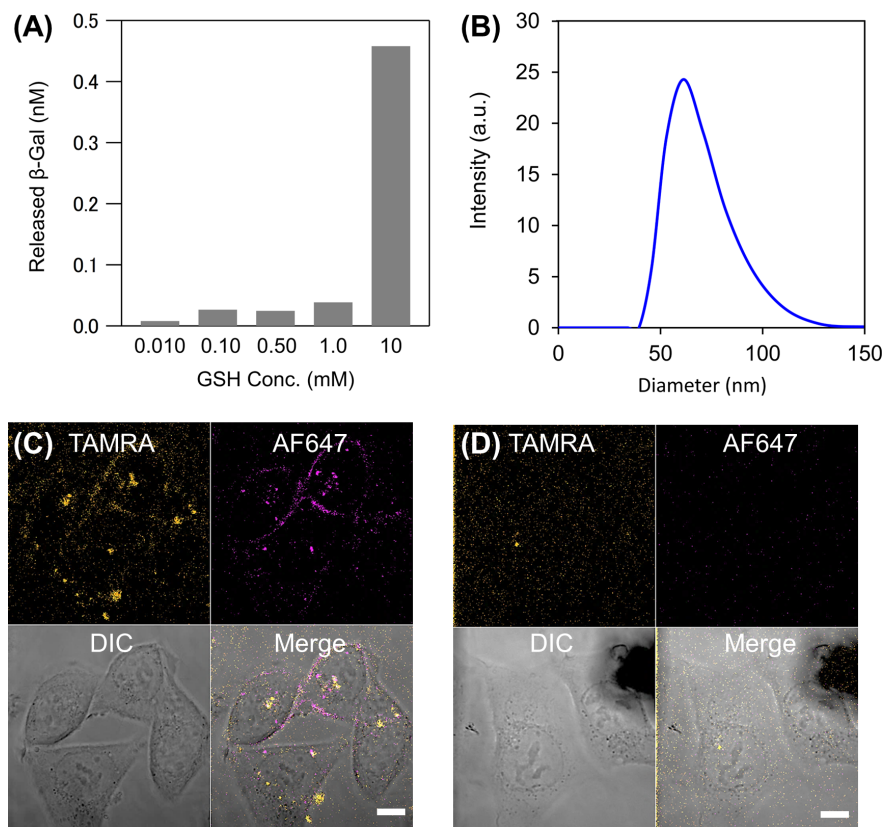


**Figure 2.** Characterization of droplets for cytoplasmic protein delivery. (A) The concentration of the released  $\beta$ -galactosidase from the droplets after incubation with various concentrations of reduced glutathione (GSH). (B) Dynamic light scattering intensity of the droplets after down-sizing using an extruder. (C) Confocal microscopic images of DLD1 cells treated with nano-droplets modified with anti-epiregulin antibody and (D) without anti-epiregulin antibody. The antibody was labeled with a fluorescent dye (Alexa Fluor 647: AF647) (pink). The nano-droplets were labeled with DPPE-PEG-TAMRA (orange). Scale bar: 10  $\mu$ m.

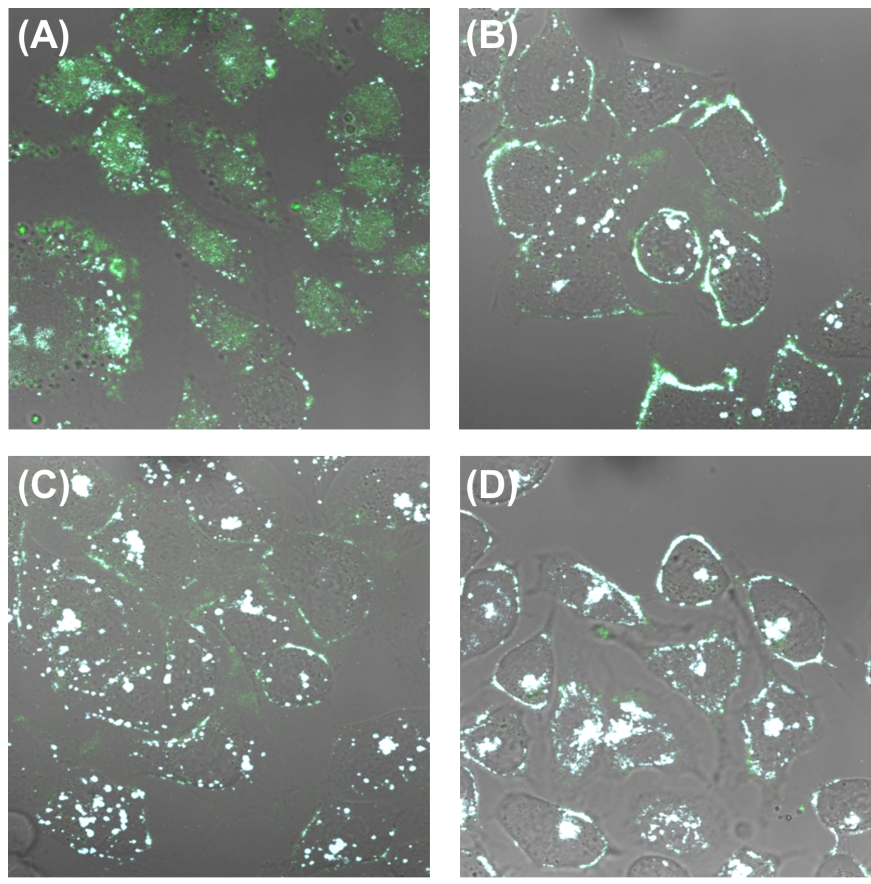


**Figure 3.** Fluorescence confocal microscopic images of cells after ultrasound-induced cytosolic delivery of  $\beta$ -galactosidase ( $\beta$ -Gal). (A) DLD1 cells treated with phase-change nano-droplets (PCNDs) carrying  $\beta$ -Gal and ultrasound, (B) those treated with  $\beta$ -Gal-carrying PCNDs without ultrasound, and (C) those treated with PCNDs not carrying  $\beta$ -Gal and ultrasound were observed after staining with a fluorescent substrate for  $\beta$ -Gal (TokyoGreen- $\beta$ Gal) and an endosomal and lysosomal staining dye (LysoTracker). (D) Intact cells were also observed as the control in the same way. The fluorescence images for TokyoGreen- $\beta$ Gal (green) and LysoTracker (cyan) were merged along with the differential interference contrast images. Scale bar: 25  $\mu$ m.

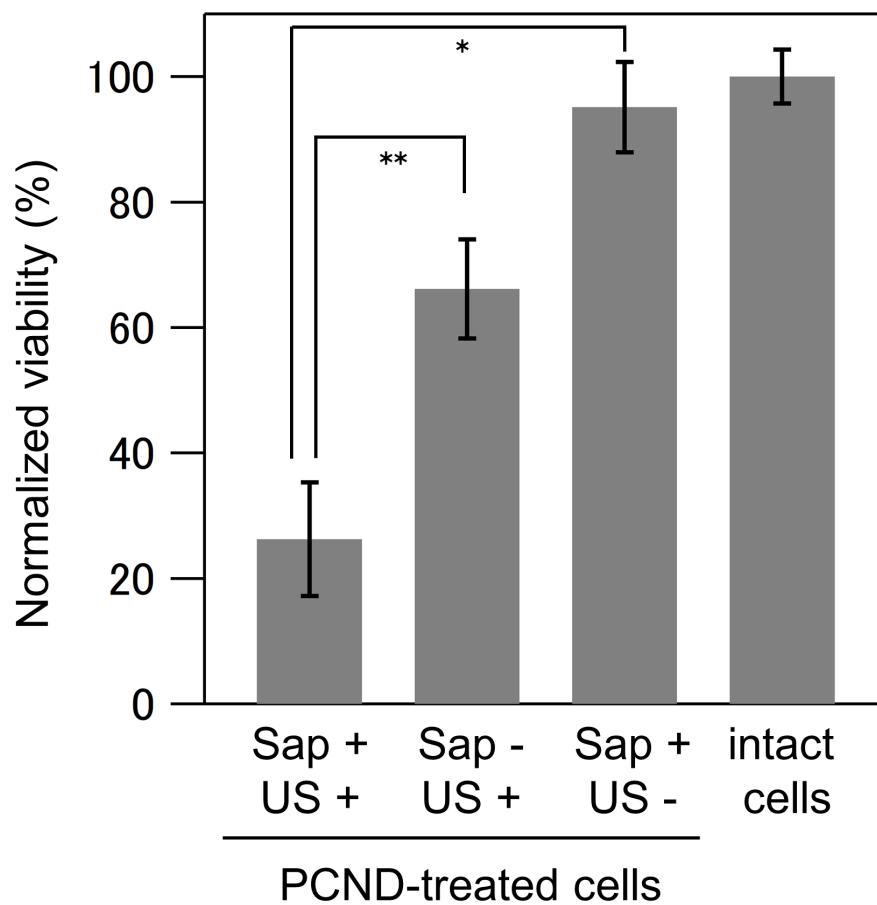


**Figure 4.** Viabilities of cells after ultrasound (US)-induced cytosolic delivery of saporin (Sap). DLD1 cells were treated with the nano-droplets (PCNDs) with or without Sap and then were exposed to ultrasound (US) or not. In the same way, the viability of intact cells was examined. The viability was normalized to that of the intact cells. Each bar represents the mean  $\pm$  S.E. ( $n = 3$ ). \* $p < 0.01$  and \*\* $p < 0.05$  versus the cells treated with both PCNDs carrying Sap and US (t-test).